JJ

INSTITUTE FOR COSMIC RAY RESEARCH

ICRR

UNIVERSITY OF TOKYO

ICRR-Report-308-94-3

Lateral Distribution of Charged Particles in Giant Air Showers above EeV observed by AGASA

S. Yoshida, N. Hayashida, K. Honda, M. Honda, S. Imaizumi, N. Inoue, K. Kadota, F. Kakimoto, K. Kamata, S. Kawaguchi, N. Kawasumi, Y. Matsubara, K. Murakami, M. Nagano, H. Ohoka, Y. Suzuki, M. Teshima, I. Tsushima, and H. Yoshii

(January 1994)

To be published in J. Phys. G: Nucl. Part. Phys. (1994)

3-2-1 Midori-cho Tanashi, Tokyo 188 Japan

Telephone (0424)-61-4131, Telefax (0424)-68-1438

Lateral Distribution of Charged Particles in Giant Air Showers above EeV observed by AGASA

S. Yoshida[1], N. Hayashida[2], K. Honda[3], M. Honda[2], S. Imaizumi[4], N. Inoue[4], K. Kadota[1], F. Kakimoto[1], K. Kamata[5], S. Kawaguchi[6], N. Kawasumi[3], Y. Matsubara[7], K. Murakami[8], M. Nagano[2], H. Ohoka[2], Y. Suzuki[1], M. Teshima[2], I. Tsushima[3], and H. Yoshii[9]

[1]*Department of Physics, Tokyo Institute of Technology, Tokyo 152, Japan*
[2]*Institute for Cosmic Ray Research, University of Tokyo, Tokyo 188, Japan*
[3]*Faculty of Education, Yamanashi University, Kofu 400, Japan*
[4]*Department of Physics, Saitama University, Urawa 338, Japan*
[5]*Nishina Memorial Foundation, Tokyo 188, Japan*
[6]*Faculty of General Education, Hirosaki University, Hirosaki 036, Japan*
[7]*Solar-Terrestrial Environment Laboratory, Nagoya University, Nagoya 464-01, Japan*
[8]*Nagoya University of Foreign Studies, Aichi 470-01, Japan*
[9]*Faculty of General Education, Ehime University, Matsuyama 790, Japan*

ABSTRACT

We have studied the lateral distribution of charged particles associated with giant air showers and the attenuation of the local particle density at 600 m from the core, S600, with atmospheric depth using data collected with the Akeno Giant Air Shower Array (AGASA). The lateral distribution at distances of more than $1km$ from the core has been observed to be much steeper than that suggested by some of the earlier measurements. The shape of the lateral distribution function has been observed to depend on the zenith angle of showers but there is no significant evidence for the dependence on the primary energy, within the resolution of the array. The systematic errors in energy estimation due to the uncertainties in the lateral distribution and the attenuation length of S600 are smaller than statistical errors. These errors have been estimated to be ~ 5 % and ~ 3 % respectively for near vertical showers with $\sec\theta = 1.1$, and ~ 10 % and ~ 12 % respectively for showers with $\sec\theta = 1.4$.

1.INTRODUCTION

An accurate determination of the energy spectrum of primary cosmic rays is of fundamental importance for understanding the origin of the highest energy cosmic rays and their propagation in galactic and/or intergalactic space. In order to estimate the energy of a primary particle with energy above 1 EeV (10^{18} eV), which initiates a Giant Air Shower (GAS) in the atmosphere, the particle density observed at a distance of $600m$ from the shower axis, S600, has been widely used as a good energy estimator (Hillas *et al.*, 1971, Dai *et al.*, 1988). In the AGASA (Akeno Giant Air Shower Array) experiment, particle density detectors consisting of plastic scintillators of 2.2 m^2 area are spread over 100 km^2 area with inter-detector separation of about 1 km (Chiba *et al.* 1992). Therefore observed particle densities are fitted to an empirical formula for the lateral distribution function (referred to as LDF hereafter) for determining S600. Since most detectors in AGASA are located at distances $R \geq 1km$ from the core, the estimated value of S600 depends sensitively on the shape of the LDF at large distances. Further, the estimated $S_\theta 600$ for a shower arriving at a zenith angle θ is first transformed to the equivalent value in the vertical direction, $S_0 600$, using the attenuation curve for S600. $S_0 600$ is then converted to the primary energy of the GAS. Therefore, a detailed understanding of the LDF for giant air showers and the attenuation of S600 with atmospheric depth is indispensable for accurately estimating the primary energy of GAS. This information is also needed for designing the detector configuration for the proposed Giant Surface Array (Cronin, 1993).

In this paper, we present our measurements on the lateral distribution of charged particles in GAS observed with AGASA and the attenuation of S600 with atmospheric depth. In Section 2, we describe the experiments performed at the Akeno Cosmic Ray Observatory to study the LDF for GAS. In Section 3, we present the observational results on the LDF for distances beyond 1 km from the shower core in some detail. In Section 4, the results obtained on the energy and the zenith angle dependence of LDF of GAS are discussed in detail. In Section 5 are presented the results of our study on the attenuation of S600 using the equi-intensity cuts on integral $S_\theta 600$ spectra. Finally, in Section 6, present results are compared with results obtained by other experiments and simulations. Based on results obtained from our study, we present a discussion on the systematic error in the estimation of S600, mainly due to uncertainties in LDF and the attenuation length of S600. We also discuss the relevance of the LDF derived from Akeno observations for estimation of primary energies of showers observed with AGASA. At the end of this Section we make a comment on the relevance of our results for possible detector configuration for the proposed Giant Surface Array (Cronin, 1993).

2.EXPERIMENTS

The very large surface array covering an area of about 100 km^2, AGASA, became oper-

ational in 1990 for studies on the highest energy cosmic rays, with energies above EeV. The details of the array have been described in Chiba *et al.* (1992). 111 density detectors are arranged with inter-detector separation of about 1 km and they are sequentially connected by a pair of optical fibers. The schematic view of the array is shown in Fig. 4. Each surface detector consists of plastic scintillators of total area of 2.2 m^2, which are viewed by a 125 mm diameter Hamamatsu R1512 photomultiplier. To measure muons associated with GAS, shielded proportional counters are deployed near 27 of the 111 surface detectors. The absorber shield consists of either a thick iron plate and a thin lead plate or concrete. The threshold energy of muons is about 0.5 GeV. AGASA is divided into 4 branches, the "Akeno Branch (AB)", the "Sudama Branch (SB)", the "Takane Branch (TB)", and the "Nagasaka Branch (NB)". The 20 km^2 array (AKENO-20), operational since December, 1984, forms a part of the AB branch (Teshima *et al.*, 1986). A data processing and storing station, called a "Branch Center", is placed at the center of each of the four branches. A new data acquisition system has been developed and installed for AGASA which makes it possible to control and operate all the surface detectors through a set of commands transmitted from the central computer at the branch center.

As a part of AKENO-20, we have a more densely arranged sub-array, called $1km^2$ array (AKENO-1) where 156 scintillators, each of $1m^2$ area, are arranged over an area of about 1 km^2, to observe primary cosmic rays with energies of $10^{15} \sim 10^{18}$ eV (Hara *et al.* 1979). This sub-array, located in the AB branch has been operational since 1981. The schematic layout for AKENO-20 and AKENO-1 arrays is shown in Fig. 1. For each of the detectors in both arrays, the photomultiplier anode signal is shaped to an exponential form with a decay constant of 10 μsec which is then discriminated to give a square pulse. The width of this pulse is proportional to the logarithm of the number of particles incident over the detector. The resultant wide dynamic range, up to $\sim 5 \times 10^4$ particles, is essential for the study of the lateral distribution of giant air showers.

3. LDF at $R > 1km$ FROM THE CORE

To determine the LDF at distances far from the core, we have used data from detectors of AKENO-1 with total detection area of 156 m^2 for showers whose core positions have been determined using data from detectors of AKENO-20. Particle densities observed in AKENO-1 detectors have been recorded using the trigger signal from AKENO-20. Since

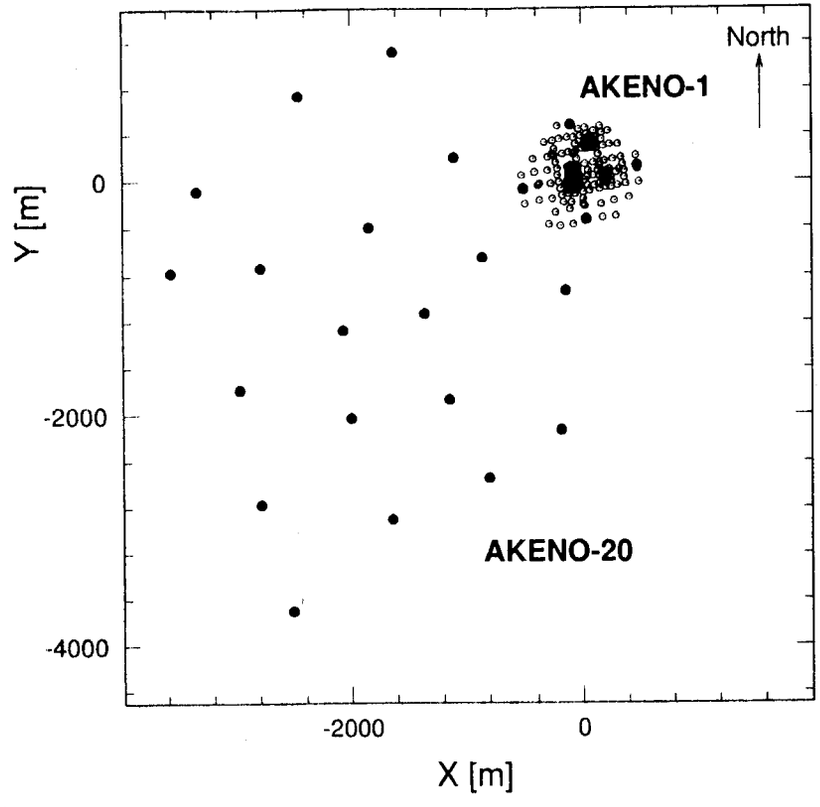

Figure 1: Schematic layout of the Akeno 20 km^2 array (AKENO-20) and the Akeno 1 km^2 array (AKENO-1). The closed circles show the density detectors, each of 2.2 m^2 area, in AKENO-20 and the open circles correspond to those of 1 m^2 area in AKENO-1.

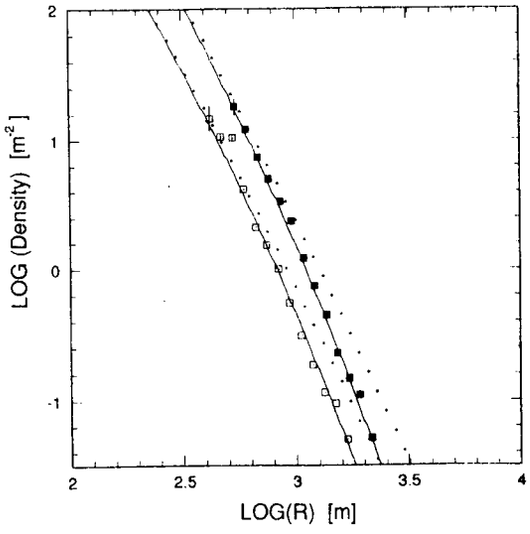

Figure 2: Lateral distribution observed by AKENO-1 for showers hitting inside the boundary of AKENO-20. The open squares show the distribution for near vertical showers with S600= 3 m^{-2} and the closed squares for near vertical showers with S600= 10 m^{-2}. The dotted curves represent the Linsley function given by Eq.(1). The solid lines represent the new lateral distribution function with an additional term as given in Eq.(2).

the accuracy in determination of the core position by AKENO-20 is about $\sim 50m$ (Nagano *et al.*, 1992), this uncertainty causes negligible effect on the determination of the LDF at distances $R \geq 1km$ from the core. In order to ensure the use of only good quality data for determination of LDF, we have used only those showers whose cores are located well inside the boundary of AKENO-20 and more than 8 detectors gave measurable signal.

Fig. 2 shows the average lateral distributions of particles, observed using detectors of both AKENO-1 and AKENO-20 arrays, for near vertical showers ($\sec\theta \leq 1.2$), for two values of S600, namely, $3m^{-2}$ and $10m^{-2}$. These S600 values correspond to primary energies of 6×10^{17} eV and 2×10^{18} eV respectively (Dai *et al.*, 1988). The dotted lines

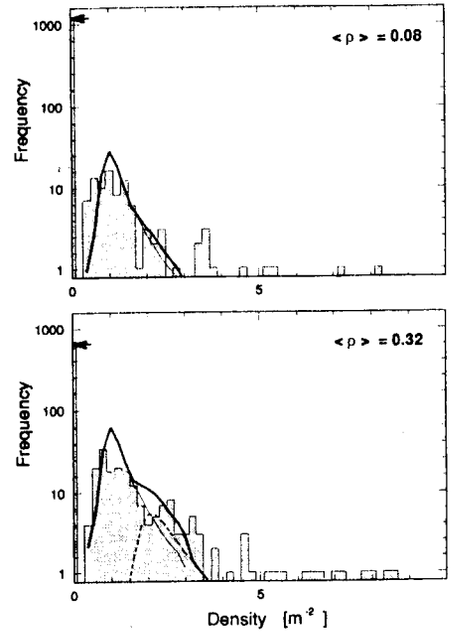

Figure 3: Density distributions for near vertical showers at distances of around 1500 $m \sim$ 2000 m from the core for two values of particle densities, $0.08m^{-2}$ and $0.32m^{-2}$ respectively. The total number of triggered detectors are 1270 ($0.03m^{-2}$) and 891 ($0.32m^{-2}$). Also shown in the figure are the expected number of detectors recording zero particles extimated from Poisson probability by the arrows. The pulse height distributions expected for one and two particles are also shown for comparison by thin solid line and dashed line. The thick solid curve shows the expected pulse height distribution taking into account the contributions of both one and two particles.

shown in Fig. 2 represent the function given by Linsley (Linsley, 1962),

$$\rho(R) = C(\frac{R}{R_M})^{-1.2}(1+\frac{R}{R_M})^{-(\eta-1.2)}, \quad (1)$$

where R_M is the Moliere unit (91.6 m at Akeno), C is a normalization factor, and η is the parameter which determines the power of LDF at $R > R_M$. η has been taken to be 3.8 for the curves shown in Fig. 2 as this was the value obtained by us from an earlier analysis (Teshima *et al.* 1986). Note that the observed lateral distribution is much steeper than that expected from Eq. (1) at distances $R > 1km$, using $\eta = 3.8$. We have examined in detail the density distributions observed at $R > 1km$ to understand this discrepancy, in particular, whether we fail to record the densities because of inappropriate recording of particle number. In Fig. 3, we show density distributions recorded in individual detectors at distances around 1.5 $km \sim 2$ km from the core, where the densities expected using the LDF given by Eq.(1) are $0.08m^{-2}$ and 0.32 m^{-2} respectively. The expected distributions from Poisson statistics are also shown in Fig. 3 for comparison. It is seen that the observed distributions are consistent with Poisson statistics for average densities of 0.08 m^{-2} and 0.32 m^{-2} taking into account detector resolution.

The observation of densities above $3m^{-2}$ may be related to the incidence of delayed neutrons (Teshima *et al.*, 1986) and will be discussed in some detail elsewhere. It is necessary to introduce an additional term in Eq. (1) to represent the steepness of the observed lateral distribution at large core distances. The best fit empirical LDF is

$$\rho(R) = C(\frac{R}{R_M})^{-1.2}(1+\frac{R}{R_M})^{-(\eta-1.2)}(1.0+(\frac{R}{1km})^2)^{-\delta}, \quad (2)$$

where $\eta = 3.8$ and $\delta = 0.6 \pm 0.1$ for near vertical showers with $\sec\theta \leq 1.2$ and energies of $6 \times 10^{17} \sim 2 \times 10^{18}$ eV.

4. LATERAL DISTRIBUTION FOR ENERGIES ABOVE 1 EeV

We have made a detailed study of the lateral distribution of particles in showers initiated by primary cosmic rays of energies above 1 EeV. We have also studied its dependence on the primary energy and zenith angle. For an individual shower, the new LDF given by Eq. (2) has been used to fit the observed densities by searching for the location of the shower core which gives the best fit. In the fitting procedure, η and C have been treated as free parameters and the value of δ has been taken as 0.6.

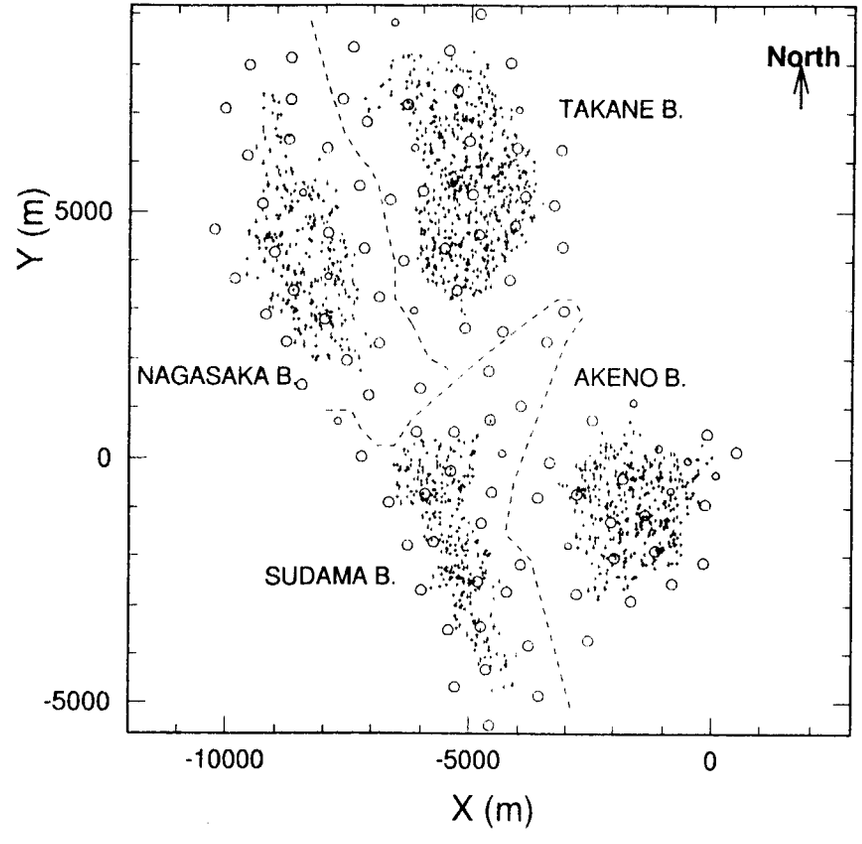

Figure 4: The core location distribution for GAS events used for the present analysis. Open circles represent the density detectors of AGASA.

Generally, in arrays designed to have a large collecting area such as AGASA (Fig. 4), the number of detectors with measurable particle density is not large enough to treat both the core location and η as free parameters for most of the observed showers. In addition, triggering bias tends to favor selection of showers with flatter LDF. Therefore, care should be taken in choosing the sample of good GAS so as to minimize the systematic errors during analysis. In order to achieve this objective for our analysis, we have used only those showers which have density information from a minimum of 8 detectors and whose cores are located well within the boundary of the array. We also require that S600 $\geq 3\ m^{-2}$. Fig. 4 shows the core location distribution for these selected showers. It may be seen that this procedure excludes all showers whose cores are located in the boundary regions of different branches. It has been observed that showers with cores in the boundary region tend to give the best fit with a steeper lateral distribution.

Next, we exclude events which possibly could suffer from large systematic errors, using a new parameter λ. This parameter λ represents the degree of goodness in locating the core position which is estimated by the maximum likelihood method. This parameter helps in selecting good GAS and discriminates against false events which occur by accidental coincidence between nearby detectors.

The likelihood function $\mathrm{L}(\rho_{LDF})$, computed for estimating the deviation from the expected LDF, is obtained by assuming that the observed densities follow the normal distribution around the densities expected from LDF, ρ_{LDF}, taking into account the expected fluctuations in density, both due to fluctuations in the cascade development and the detector resolution. This fluctuation has been determined experimentally (Teshima *et al.*, 1986). The search for S600 and core position in the fitting procedure is carried out through maximizing $\mathrm{L}(\rho_{LDF})$, based on the Maximum Likelihood Estimation (MLE).

We also calculate similar likelihood function $\mathrm{L}(\rho_{BG})$ taking the events as accidental ones. Since the false events are recorded by accidental coincidence of the cosmic ray muons in the AGASA experiment, the flat lateral distribution of the particle density is assumed to estimate $\mathrm{L}(\rho_{BG})$.

Our new parameter λ, the maximum likelihood ratio is defined as

$$\lambda = \log \frac{\mathrm{L}_{max}(\rho_{LDF})}{\mathrm{L}(\rho_{BG})}. \qquad (3)$$

where $\mathrm{L}_{max}(\rho_{LDF})$ is the maximum value of $\mathrm{L}(\rho_{LDF})$ obtained by MLE. The greater th

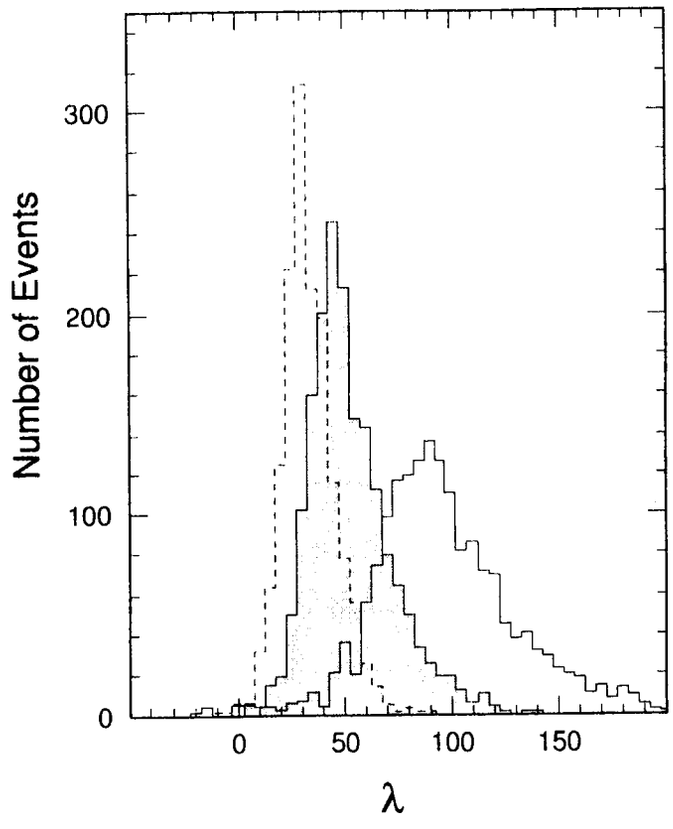

Figure 5: λ distribution for simulated events for 3 ranges of S600. The broken line corresponds to $0.8 \leq \log(S600) \leq 1.0$. The solid line with shaded area corresponds to $1.8 \leq \log(S600) \leq 2.0$. The solid line with empty region corresponds to $2.6 \leq \log(S600) \leq 2.8$.

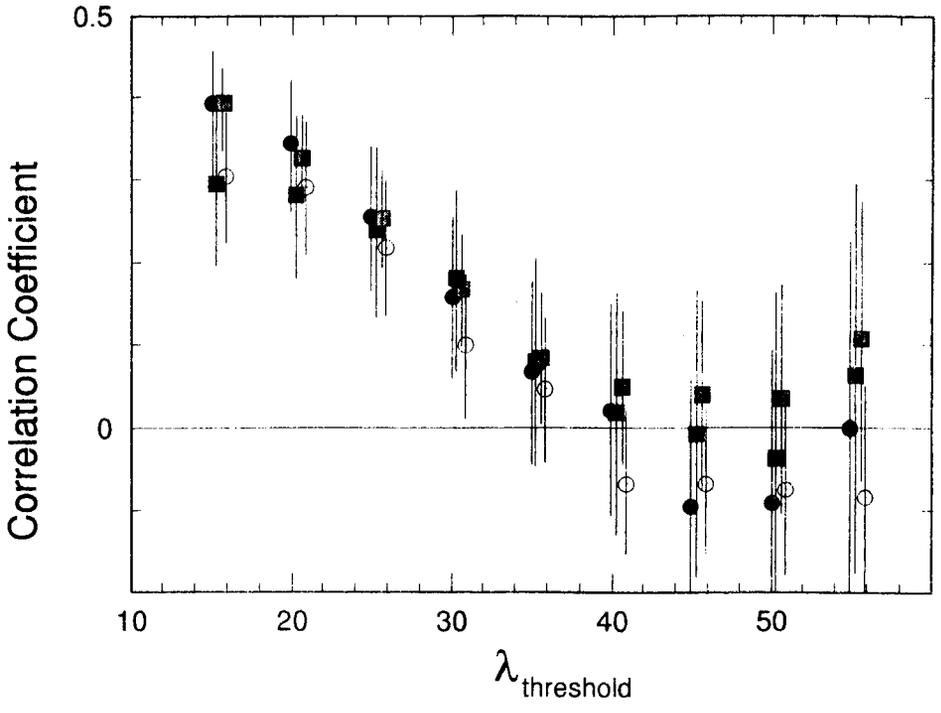

Figure 6: The correlation coefficient between λ and η for observed events and simulated events for three different η values with $\lambda \geq \lambda_{threshold}$. The closed circles correspond to simulated events with $\eta = 3.8$, the closed squares correspond to those with $\eta = 4.2$, and the shaded squares correspond to those with $\eta = 4.0 - 1.6(\sec\theta - 1)$. The open circles correspond to observed events. λ and η should be independent and the correlation coefficient should be 0 unless there is some bias in the fit of observed densities to the LDF.

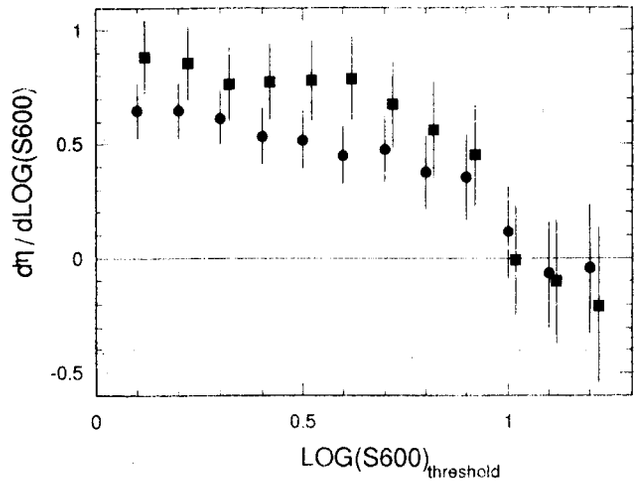

Figure 7: Apparent energy dependence, $d\eta/d\log$ S600 for events simulated by Monte Carlo method under assumption of constant η. η is assumed to be 3.8 (closed circles) and 4.2 (closed squares) respectively. There should be no energy dependence of η in the bias free region.

value of λ is, the more likely that the events are identified as real showers. Fig. 5 shows the λ distributions for events with three S600 values which have been simulated by the Monte-Carlo method. It is clearly seen that lower energy events have smaller λ, which means that the fraction of "poorly fitted" events is large. Events with small λ tend to be fitted with a flatter LDF systematically due to relatively larger Poisson fluctuations in densities and the smaller number of detectors triggered within $\sim$ 600 m from the shower axis. This leads to a positive correlation between λ and determined η. In Fig. 6 are shown the correlation coefficients between λ and η for both the observed events and simulated events with $\lambda \geq \lambda_{threshold}$. Three different values of η were assumed for simulated events. Fig. 6 shows the near absence of correlation for events with $\lambda \geq 35$. This suggests that there is very little systematic bias affecting the fit to the LDF for showers with $\lambda \geq 35$.

In addition to this criteria, we must also examine the threshold primary energy ($S_{threshold}600$) above which the systematic error due to the triggering bias is negligible. Even if only the events with $\lambda \geq 35$ are selected, events with flatter lateral distribution than the average are triggered more efficiently near the threshold energy. This is due to the fact that events with flatter lateral distribution tend to give small but finite density in a larger number of detectors. This bias would cause an artificial energy dependence of η. To verify this possibility, we simulated events assuming a constant value of η by Monte-Carlo method and analyzed these showers with η as a free parameter. In this analysis, we select showers with the same criterion as described above for core positions, that is, the number of triggered detectors (≥ 8), and $\lambda \geq 35$. Fig. 7 shows the S600 dependence of $d\eta/d\log S600$ obtained, for simulated events with $\eta = 3.8$ and 4.2 with S600 $\geq$ S600$_{threshold}$. It is seen from this figure that events with S600 smaller than 10 m^{-2} have positive energy dependence. This means that a flatter LDF than the real one gives the best fit for lower energy events. Thus, we use only those showers which have $\lambda \geq 35$ and S600 $\geq 10\ m^{-2}$ for the following lateral distribution analysis. Note that for showers arriving vertically, S600$\geq 10\ m^{-2}$ corresponds to E $\geq 2 \times 10^{18}\ eV$. The number of showers selected with these criteria is 290. For an individual event, we determine η by fitting observed densities to the LDF represented by Eq. (2) with C and core location as free parameters and maximizing $L(\rho_{LDF})$.

The η values determined for the observed GAS sample, selected as specified above, are plotted as a function of S600 for near vertical showers ($\sec\theta \leq 1.1$) in Fig. 8(a). The zenith angle dependence of η is shown in Fig. 8(b). Each dot corresponds to a η value determined from $L_{max}(\rho_{LDF})$ for a shower. From the analysis of simulated events with a constant η, the dispersion in η values seen in these two figures, 8(a) and 8(b), is consistent with the effect of resolution in η determination with AGASA and it does not reflect fluctuations in cascade development. It is seen that the dependence of η on S600 is very weak while η depends strongly on the zenith angle of the shower. The zenith angle and S600 dependence of η have been determined by the Least Square Method on the $\sec\theta$ S600 plane. For S600 $\geq 10\ m^{-2}$ and $\sec\theta \leq 1.7$, η can be expressed as

$$\eta = (4.02 \pm 0.18) - (0.11 \pm 0.43)\log\frac{S600}{10m^{-2}} - (1.87 \pm 0.54)(\sec\theta - 1). \qquad (4)$$

Errors have been assigned based on the confidence level of 99.5% given by F-distribution. Since the dependence of η on S600 is much smaller than the errors, η can be approximated

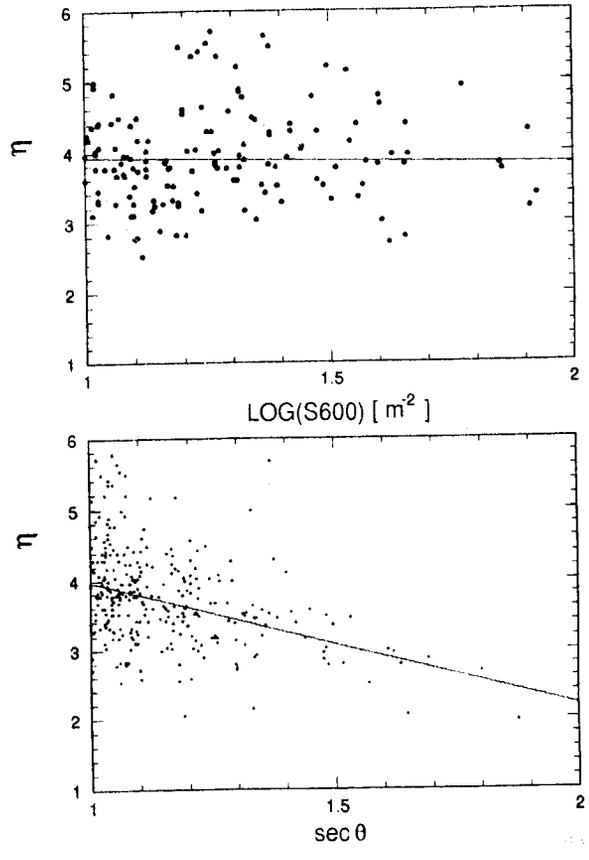

Figure 8: η vs S600 for near vertical showers with $\sec\theta \leq 1.1$ (a), and η vs $\sec\theta$ for showers with S600 $\geq 10\ m^{-2}$ (b). The solid line shows the best fit line using the least square method.

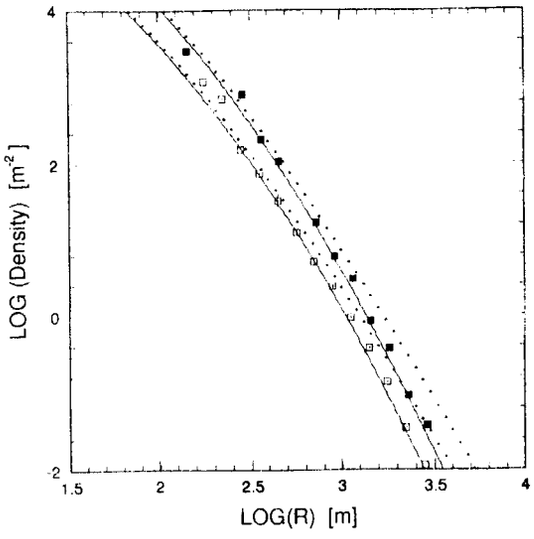

Figure 9: Average lateral distributions for near vertical showers, $\sec\theta \leq 1.1$ determined using data from AGASA. The open squares show the distribution for showers with S600= 10 m^{-2} and the closed squares for showers with S600= 30 m^{-2}. The dotted curves represent the empirical formula obtained by Teshima *et al.* (1986).

as

$$\eta = (3.97 \pm 0.13) - (1.79 \pm 0.62)(\sec\theta - 1). \quad (5)$$

for 10≤S600≤100 m^{-2} and $\sec\theta \leq 1.7$. For showers of $\sec\theta = 1.1$, η becomes 3.79 ± 0.09 which agrees well with the LDF observed with AKENO-1 as described in Section 3.

Fig. 9 shows the average lateral distribution determined by AGASA as discussed above. It is seen that the new LDF curve given by Eq. (2) with η given by Eq. (5) gives a good fit for the observed densities.

5. ATTENUATION CURVE OF S600

In order to estimate primary energies of showers arriving at different zenith angles, we must know the attenuation of GAS with atmospheric depth. Since we use $S_\theta 600$ as an

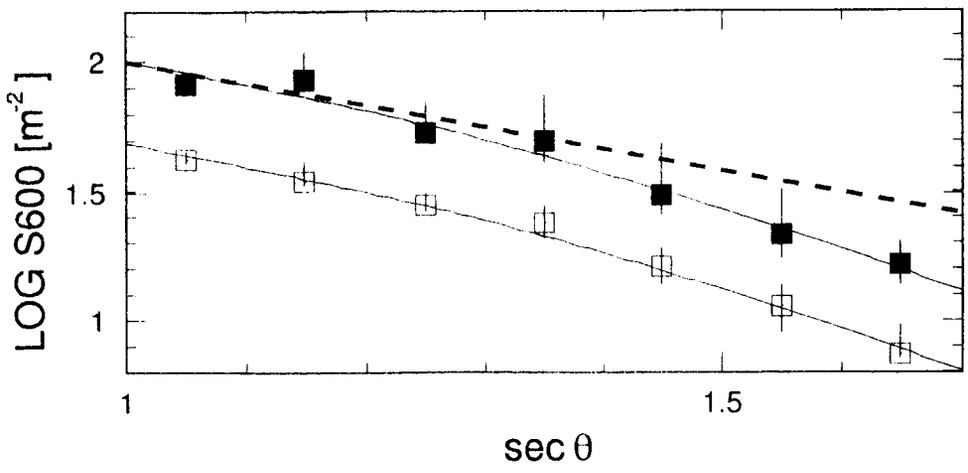

Figure 10: The variation of S600 with zenith angle obtained using the method of "equi-intensity cuts". The solid curves correspond to the most probable attenuation curve represented by Eq.(7) derived from integral S600 spectra. The dashed line represents the attenuation curve used in AKENO-20 array experiment and given by Eq.(6).

energy estimator, the attenuation curve of S600 must be experimentally determined.

We determine the attenuation curve of S600 by "equi-intensity cuts" on the integral $S_\theta 600$ spectra, based on the assumption that the flux of showers above certain primary energy does not change with atmospheric depth. For this analysis, we use S600 obtained from the LDF using the parametrization given in Eqs. (2) and (5). Fig. 10 shows the attenuation curves of S600 for two different intensities. The primary energies are about 9×10^{18} *eV* and 2×10^{19} *eV* respectively. In this energy region, AGASA has almost 100% detection efficiency, irrespective of zenith angles, and systematic errors are negligible as discussed above. The dashed line represents the attenuation curve obtained from data

collected with the AKENO-20 array (Nagano *et al.*, 1992) and is represented by

$$S_\theta 600 = S_0 600 \exp[-\frac{X_0}{\Lambda_{att}}(\sec\theta - 1)] \quad (6)$$

where the attenuation length Λ_{att} is 500 g/cm^2 and X_0 is the atmospheric depth at Akeno (920 g/cm^2). For showers with $\sec\theta < 1.4$, this equation agrees with the measurements with AGASA, but it deviates significantly for $\sec\theta > 1.4$. By adding a second term of $\sec\theta$, the new relation may be expressed as :

$$S_\theta 600 = S_0 600 \exp[-\frac{X_0}{\Lambda_1}(\sec\theta - 1) - \frac{X_0}{\Lambda_2}(\sec\theta - 1)^2] \quad (7)$$

$$\Lambda_2 = 594^{+\ 268}_{-\ 120}\ g/cm^2$$

Here, Λ_1 is determined to be 500 g/cm^2 to give the best fit. The error quoted above is at a confidence level of 68 % and has been evaluated through Monte Carlo simulations taking fluctuations in the number of events into account.

6. DISCUSSION

6.1 Comparison with other experiments

The LDF given by Eq. (1) derived by Linsley (1962) is widely used in GAS experiments. Our present results show that the lateral distribution of charged particles at $R > 1km$ from the core is much steeper than Eq.(1). By selecting only near vertical showers with cores incident well inside the Volcano Ranch array, which are printed in Catalogue (Linsley 1980), we have made a comparison with the present experiment after taking into account the difference in the values of Moliere units between Volcano Ranch and Akeno. It is found that there is a difference between the experimental points between the two experiments for distances larger than 1 km from the core. Though the thickness of scintillators and the container boxes and also the observation levels are different, it is not easy to explain the difference in observed densities at far distances from the core only in terms of these differences. Since the density at large distances from the core is less than $1/m^2$, the number of detectors without any signal is rather large. In such cases, it is important to examine the distribution of the number of particles in detectors located at large distances as shown in Fig. 3.

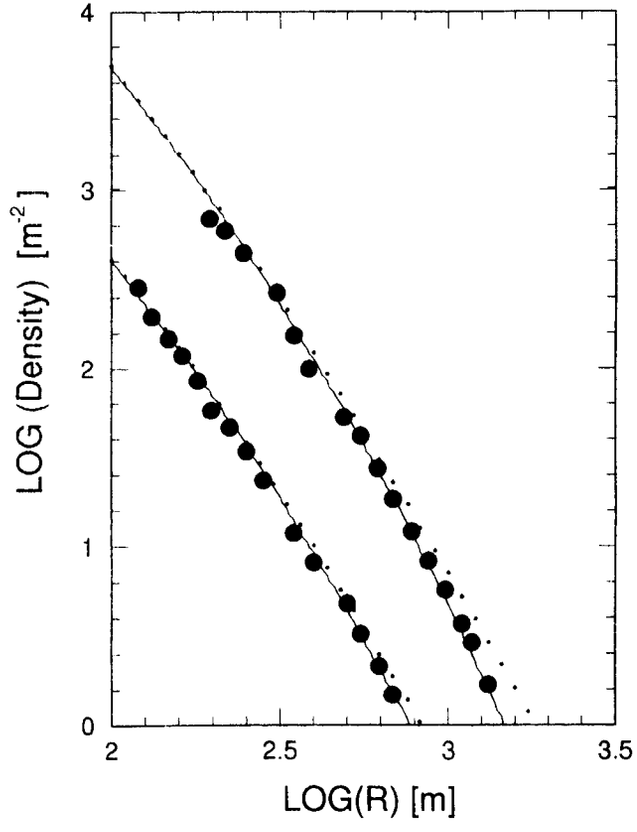

Figure 11. Average lateral distribution observed with the Yakutsk array for $\theta = 32°$. The primary energies for the two distributions shown are 1.5×10^{19} eV and 1.6×10^{18} eV respectively. The solid curves represent the new LDF given by Eq.(2) corresponding to Yakutsk altitude. The small dots show the Linsley LDF given by Eq.(1).

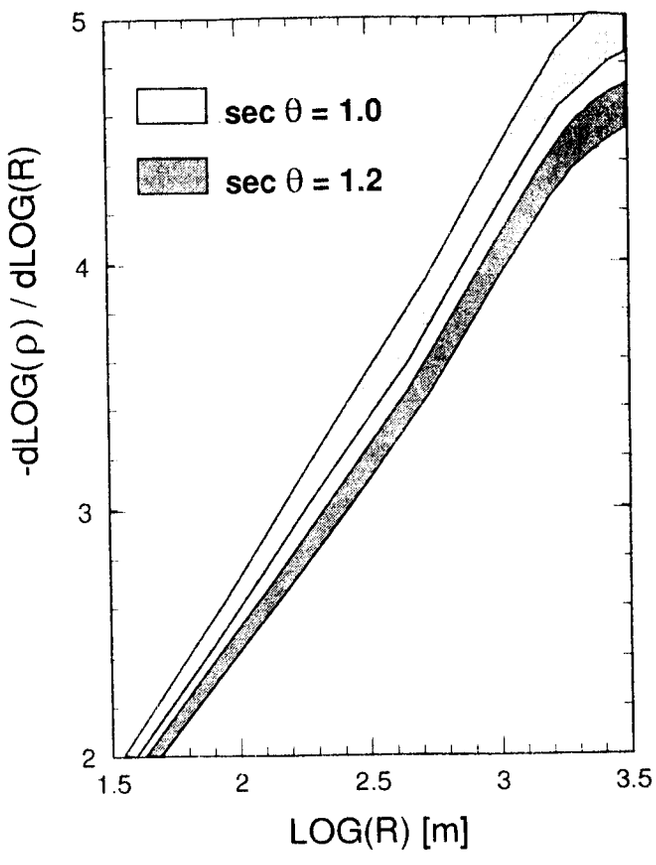

Figure 12: Local slope $d\log\rho/d\log R$ of the lateral distribution function, Eq.(2), as a function of the core distance taking into account the error in η determination.

The Yakutsk group has also reported the lateral distribution of charged particles as observed with their surface array (Efimov *et al.*, 1991). Fig. 11 shows the average lateral distributions for events with 1.5×10^{19} eV and 1.6×10^{18} eV at $\theta = 32°$ observed by the Yakutsk array. The curves representing Eqs. (1) and (2) at the corresponding atmospheric depth are also shown in the figure. It is seen from Fig. 11 that the lateral distributions observed at Yakutsk are well represented by the LDF, Eq.(2), obtained from AGASA data. In their study of the LDF, the Yakutsk group uses Eq. (1) and a significant energy dependence of η has been reported. The rate of change of η with energy, $d\eta/d\log E$ is 0.26 while no significant energy dependence of η has been observed in Akeno data. This difference is not very large when compared with the error in the measurement of η as given by Eq.(4). However, it is relevant to make some comments on the study of the energy dependence of LDF. Firstly, the core locations which give the best fit have strong correlation with the assumption of η as described in Section 4. Therefore, a careful treatment is required to remove this systematic effect as has been carried out by us in Section 4; otherwise artificial energy dependence is likely to be produced. Secondly, we must consider the dependence of the slope of the lateral distribution on the core distance. The local slope of Eq.(2) derived from our experiments, $d\log\rho/d\log R$, is shown in Fig. 12 as a function of the core distance. It is seen that the local slope becomes larger with increasing core distance. Thus the gradual steepening of the LDF with distance causes the *apparent* energy dependence of LDF, because with larger and larger primary energy, the more and more distant region from core can be observed. Therefore, it is advisable that the range of core distance must be kept constant when examining the energy dependence of the lateral distribution.

6.2 Comparison with the simulated lateral distribution

Cronin (1993) has shown lateral distributions of gammas, electrons/positrons and muons between 100 m and several kilometers from the core for showers initiated by 10^{19} eV proton, iron and gamma ray, based on simulations carried out using the "MOCCA" program developed by Hillas (Hillas 1992). Fig. 13 shows the comparison of simulated lateral distribution of charged particles (electrons/positrons and muons) in showers initiated by 10^{19} eV protons with the Akeno LDF, Eq. (2), between 500 m and 3 km from the core. It is interesting that the simulated lateral distribution given by "MOCCA" for 10^{19}eV showers

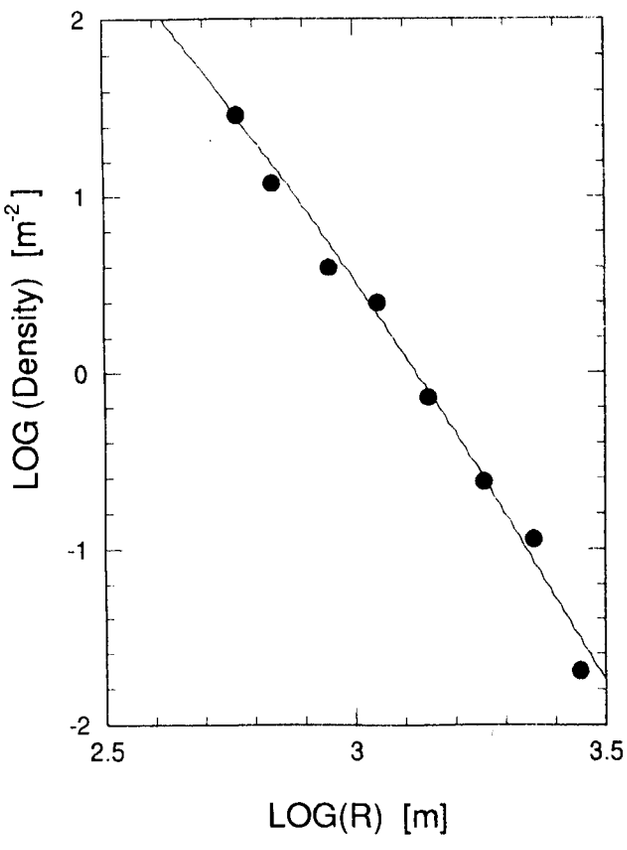

Figure 13: Comparison of the average lateral distribution for showers (closed circles) obtained from simulations using the "MOCCA" program with the new LDF curve, Eq.(2), for an atmospheric depth of 1000 g/cm^2. The simulation points are normalized to a primary energy of 5×10^{18} eV.

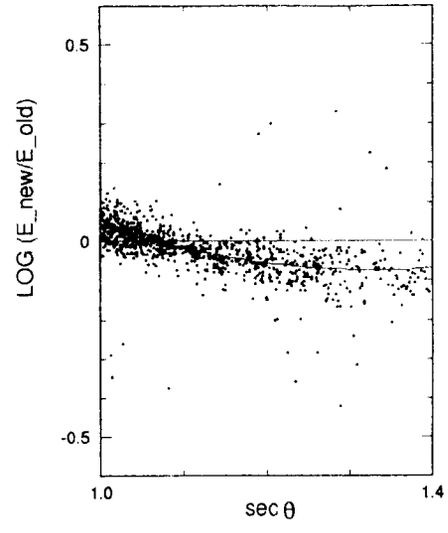

Figure 14: Scatter plot of the ratio of primary energy determined using the new LDF and the new attenuation curve to energy determined using the procedure followed earlier (Nagano et at. 1992), as a function of zenith angle. The best fit curve is also shown in the figure.

agrees well with the experimental LDF even at distances larger than 1 km and may be used fruitfully and with confidence for designing the proposed giant surface array.

6.3 Effect of the new LDF and new attenuation curve on energy determination

So far we have used Eq. (1) with constant η, which is independent of zenith angle, to determine $S_\theta 600$ and Eq. (6) to convert from $S_\theta 600$ to $S_0 600$ in AGASA experiment, since the number of events were not large enough to determine the zenith angle dependence of η. Now it is necessary to examine the difference in energies estimated using the new LDF and the new attenuation curve with values obtained using the old LDF and the attenuation length used earlier. Fig. 14 shows the ratio of energy estimated using the new LDF and the attenuation curve to energy obtained using the earlier method, as a function of the zenith angle for observed events with $E \geq 10^{18}$ eV.

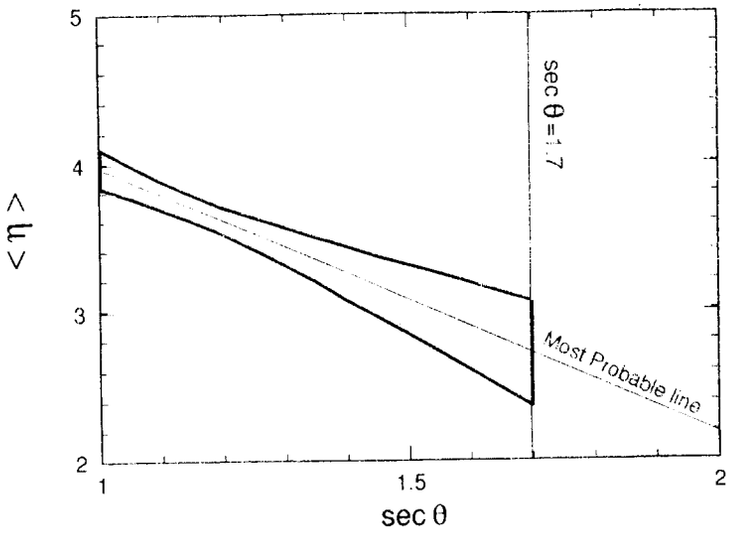

Figure 15: The allowed region for the average value of η at the 99.5 % C.L. obtained using the F-distribution, as a function of zenith angle. The line representing the average value of η is also shown.

It is seen that the ratio decreases with increasing zenith angle. The average change in energy is about +10% for near vertical showers and about -15% for showers with $\theta = 45°$.

6.4 Uncertainty in the energy estimation of showers due to the limited accuracy in determination of η and the attenuation curve of S600

The allowed region of average $\eta(\sec\theta)$ derived from a linear fit of the η dependence on zenith angle is shown in Fig. 15. This region represents the uncertainty in determination of the most probable value of η for a given zenith angle. To check for the systematic deviation of the estimated S600 due to this uncertainty in the LDF, we fit the observed GAS events to LDF with η varying within the allowed region. The average deviation in the value of S_0600 obtained in this way is shown in Fig. 16 as a function of the zenith angle. The systematic deviation in S_0600 due to the uncertainty in the LDF is $\sim \pm 5\%$ for

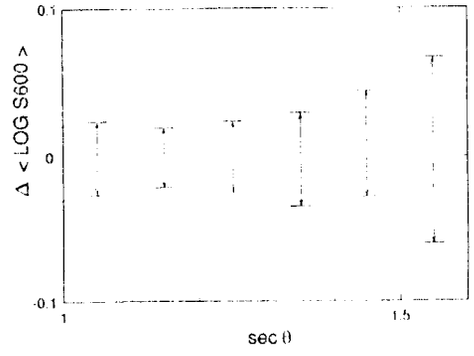

Figure 16: The deviation of S600 due to the uncertainty in η.

near vertical showers, $\sim \pm 10$ % for showers with $\sec\theta = 1.4$, and $\sim \pm 20\%$ for showers with $\sec\theta = 1.6$. The systematic deviation in energy estimation due to the limited accuracy of the attenuation curve of S600 has also been evaluated. In Fig. 17 is shown the probable uncertainty in the estimated value of S_0600 after conversion from $S_\theta 600$ as a function of zenith angle. Though the error in A_2 represented by Eq. (7) is not so small, the average shift in the energy estimate is limited to within ± 20 %. If we select showers with zenith angles smaller than 45°, the probable systematic uncertainty in energy estimation due to both the uncertainty in the LDF and the attenuation curve is estimated to be no more than ± 10 % (for $\sec\theta = 1.1$) and ± 20 % (for $\sec\theta = 1.4$), even if both the systematic errors shift the estimated energy in the same direction. It may be mentioned here that other errors in the determination of S600, such as statistical and core determination errors, have been estimated to be larger than these errors. These errors will be discussed in detail in the paper on the energy spectrum which is under preparation.

6.5 Comments on detector configuration for the proposed Giant Surface Array

Construction of a Giant Surface Array covering an area of about 5,000 km^2 has been proposed by Cronin (1993) to study the energy spectrum of primary cosmic rays in the energy range, $10^{19} \sim 10^{21}$ eV, with good statistics to be collected over a few years. There is tremendous astrophysical interest in this energy range from the point of view of acceleration

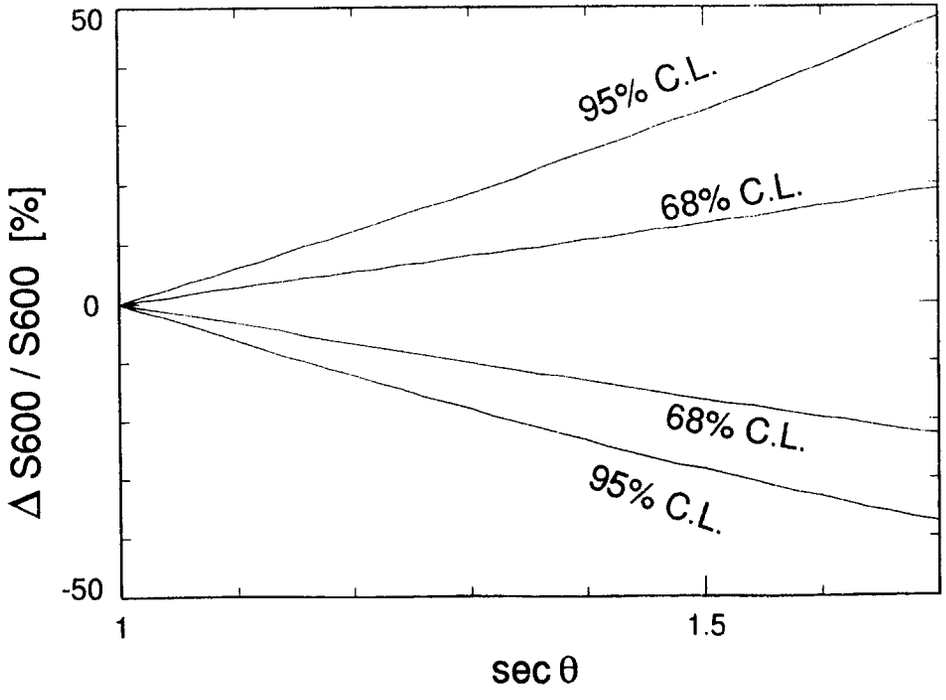

Figure 17: Probable uncertainty in S600 estimation due to the error in estimation of attenuation curve of S600. The confidence level shown for each curve has been evaluated through Monte Carlo simulation.

and propagation of these extremely energetic particles in the interstellar and intergalactic space. Design considerations for detectors for this array and possible detector configurations have been discussed extensively in several Workshops and Conferences, Paris (April, 1992), Adelaide (January, 1993), Calgary (July, 1993) and Tokyo (September, 1993).

The size of detectors and their separation depends much on the lateral distribution of shower particles. In case the detector spacing is 1.5 km as under consideration now (de Souza et al, 1992), the typical distance between observed density points is about 1 km. As discussed above, at a distance of 1 km from the core, the charged particle density in a GAS, estimated using Eq. (2) is $\sim$ 65% compared to the density expected from Eq. (1). This relatively large difference in particle density has important implications for the area of detectors suitable for use in the Giant Surface Array.

ACKNOWLEDGEMENT

We are grateful to Akeno-mura, Nirasaki-shi, Sudama-cho, Nagasaka-cho, Takane-cho and Ohoizumi-mura for their kind cooperation. We also wish to acknowledge the valuable help given by other members of the Akeno Group in the construction and maintenance of the array.

We thank Prof. S. Tonwar of Tata Institute of Fundamental Research for his careful reading of the manuscript and many valuable suggestions. The data analysis was partly performed on the computer M780 at the Institute for Nuclear Study, University of Tokyo.

REFERENCES

Chiba N, Hashimoto K, Hayashida N, Honda K, Honda M. Inoue N, Kakimoto F, Kamata K, Kawaguchi S, Kawasumi N, Matsubara Y, Murakami K. Nagano M, Ogio S, Ohoka H, Saito To, Sakuma Y, Tsushima I, Teshima M, Umezawa T, Yoshida S and Yoshii H 1992, Nucl. Instrum. Methods **A311** 338

Cronin J W 1992, University of Chicago preprint, **EFI 92-08**

Cronin J W 1993, in the Invited Talk at Tokyo Workshop for Study of the Extremely High Energy Cosmic Rays.

Dai H Y, Kasahara K, Matsubara Y, Nagano M, and Teshima M 1988 J.Phys.G: Nucl.Phys. **14** 793

de Souza K, Gillman M, Hart S, Lloyd-Evans J, McMillan J E and Watson A A 1992 Nucl.Phys B (Proc.Suppl.) **28B** 135

Efimov N N, Efremov N N, Glushkov A V, Makarov I T, Petrov P D and Pravdin M I 1991 Proc. 22nd ICRC, Dublin **4** 339

Hara T et al. 1979, Proc.16th ICRC, Kyoto **8** 135

Hillas A M, Marsden D J, Hollows J D and Hunter H W 1971, Proc.12th ICRC, Hobart **3**, 1001.

Hillas A M 1992 Nucl.Phys B (Proc.Suppl.) **28B** 67

Linsley J et al. 1962, J.Phys.Soc.Japan **17** Suppl A-III 91

Linsley J 1980, Catalog of Highest Energy Cosmic Rays **1**,*World Data Centre C2 for Cosmic Rays* edited by M Wada

Nagano M, Teshima M, Matsubara Y, Dai H Y, Hara T, Hayashida N, Honda M, Ohoka H and Yoshida S 1992, J.Phys.G: Nucl.Part.Phys. **18** 423

Teshima M, Matsubara Y, Hara T, Hayashida N, Honda M, Ishikawa F, Kamata K, Kifune T, Mori M, Nagano M, Nishijima K, Ohoka H, Ohno Y and Tanahashi G 1986, J.Phys.G: Nucl.Phys. **12** 1097